551.511.2

THE INTERACTION OF THE MONTHLY MEAN FLOW AND LARGE-SCALE TRANSIENT EDDIES IN TWO DIFFERENT CIRCULATION TYPES

Part I: The forcing effect of large-scale turbulence and kinetic energy balance

by

HANNU SAVIJÄRVI

Department of Meteorology
University of Helsinki

Abstract

Diagnostic distributions for some of the kinetic energy balance terms and the forcing effect of large-scale turbulence on the time mean flow are presented in high-index and low-index (blocking) circulation types, both for one-month periods. Calculations are based on NMC numerical height analyses above 850 mb through geostrophic wind approximation. The results indicate no large differences in the forcing patterns in these two very different flow types.

The kinetic energy balance conditions for both the time-mean flow and the transient part are found to be longitudinally variable and no terms presented can be generally eliminated as small. The third order term is presented and discussed.

1. *Introduction*

Understanding and modelling the climate and the general circulation of the atmosphere is a challenging and urgent task for contemporary meteorology. One step toward this goal is to study the statistics collected on climatological variables and the time-mean balance conditions of the related dynamical variables; the balance conditions observed give useful information for modelling purposes and serve as empirical verification for the model results.

At present the atmospheric conditions averaged zonally are generally well-known (*e.g.* OORT & RASMUSSON, [10]) and satisfactorily modelled (SALTZMAN &

VERNEKAR, [11]). The next logical step is to account for the longitudinal differences observed and their sensitivity to the mean flow variations. This is clearly crucial for good parameterization of the transient phenomena in the two or three-dimensional statistical-dynamical (SD) climate models.

The forcing effect of the transient eddies (»large-scale turbulence») on the time mean flow is not yet adequately known. This interaction clearly depends on the averaging period, diagnostic studies hitherto having been based mainly on yearly mean periods including seasonal variations. The SD models will probably use shorter averages, however, with one month or season being a natural time step (WILLSON, [13]).

The global energy cycle of the atmosphere is generally well-known (OORT & PEIXOTO, [9]), but the local kinetic energy balance which must then include the important transport processes, has not been studied as extensively.

The present study focuses partly on the three-dimensional structure of the horizontal forcing effect caused by the large-scale turbulence on the mean flow, and partly on the local kinetic energy balance in the time domain. The time-averaging period for mean value $\bar{f}$ is one month and the transients $f' = f - \bar{f}$ thus include travelling cyclones and other synoptic systems but not yearly variations or small-scale turbulence. The calculations were made for two different flow types: a high zonal index period and a low index (strong blocking anticyclone) period. The results thus interpret the sensitivity of the forcing and the kinetic energy balance to the changes in the mean flow patterns.

2. *Data*

The calculations are based on NMC numerical height analyses and are made in the conventional NMC octagonal grid on a polar stereographic map projection (mesh width 381 km at 60°N; 1977 grid points) using centred differences. The winds are geostrophic approximations. Finally the vector quantities were transformed into (λ, φ) components for clearer presentation.

Two different circulation types were selected subjectively from the data files to present a typical rapid west-to-east basic flow with cyclone activity (»high-index case») and a strong stationary anticyclone accompanied by low zonal index (»blocking case»). The vertical means of the time-averaged height fields for the two cases are shown in Fig. 1. The high-index case covers the period 1–31.12.1965 (12/65) with two daily analyses at nine pressure levels (85–70–50–40–30–25–20–15–10 cb). The monthly mean height field is quite a typical winter mean field. The »blocking case» includes the period 28.1–28.2.1965 (2/65), with two

daily analyses at five levels (85–70–50–30–20 cb). The blocking anticyclone stayed west of the British Isles for the whole period, retreating somewhat to Iceland at the end of February. The mean height field clearly shows the blocking centre which was noticeable at all five pressure levels. References to this particular episode are made *e.g.* by STARK [12], MURRAY [6] and PERRY [7].

A crucial point in all studies concerning averages is naturally what is meant by the averaging procedure and the fluctuations around the mean. In this study the one-month time mean value is the arithmetic mean of all observations at a grid point. The periods were selected to be steady in the sense that the trends in the mean values were small. The simple arithmetic mean is then expected to be representative of the »average» conditions for the period. The fluctuations, *i.e.* transient eddies, include all time scales from the resolution limit up to one month and are due to different physical reasons. However, the main sources are the travelling synoptic scale weather systems in about 3–5 day periods.

All the geographical distributions shown are vertical averages between 850 mb and 100 mb (200 mb for the blocking case), so they do not contain boundary layer phenomena. The high-index case results are also shown as mean meridional cross-section to reveal the vertical structure.

3. *Results*

3.1 The nonlinear interaction field

The mean fields are determined by the primitive equations of atmospheric motion averaged appropriately. For horizontal flow the local time mean momentum balance can be written as

$$\frac{\partial \bar{V}}{\partial t} = -(\bar{V}\cdot\nabla)\bar{V} - \bar{\omega}\frac{\partial V}{\partial p} - \nabla g\bar{z} - fk\times\bar{V} + \bar{F} + A_H - \frac{\partial}{\partial p}\overline{\omega' V'} \qquad (3.1)$$

scale (ms^{-2})	10^{-6}	10^{-4}	?	10^{-3}	10^{-3}	?	10^{-4}	?

where the scales for the terms refer to mid-tropospheric values for monthly mean conditions according to this study (rms-values over the grid). The local change in the mean horizontal wind is small compared with the forces, which thus have to balance each other. The forces are the mean advection (horizontal and vertical) of the mean flow, the mean pressure gradient force, coriolis force and the averaged effect of small-scale turbulence. The last two terms are due to the transient large-

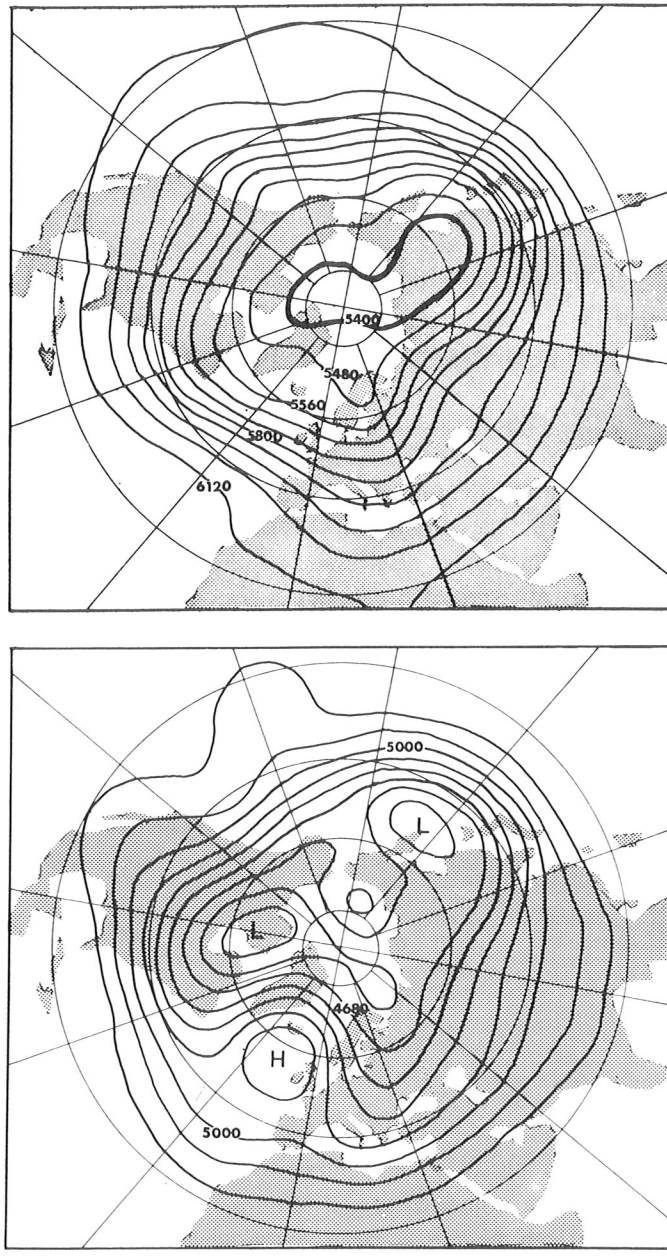

Fig. 1. Monthly mean height fields $\bar{z}$ averaged vertically for the two periods in 1965. Unit: m.

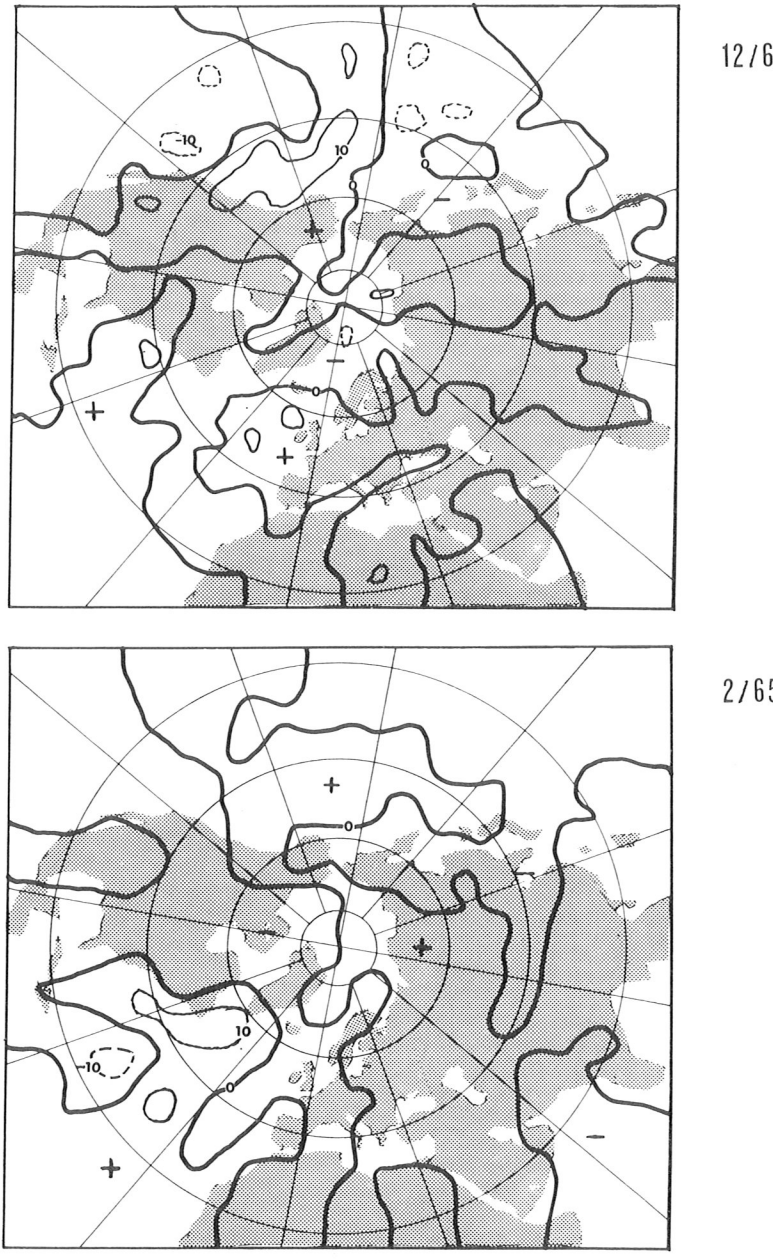

Fig. 2. Zonal component A_λ of the horizontal forcing term averaged vertically. Unit: 10^{-5} m s^{-2}.

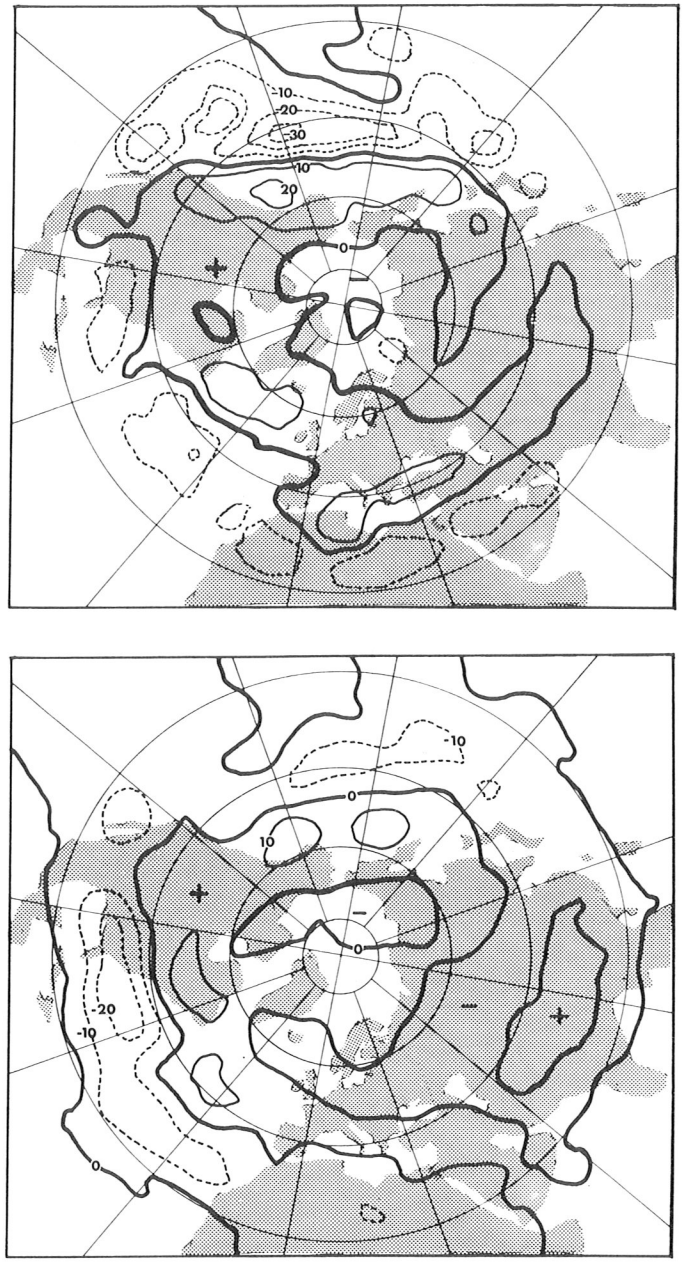

Fig. 3. Meridional component A_φ of the horizontal forcing term averaged vertically. Unit: $10^{-5}\,\mathrm{m\,s^{-2}}$.

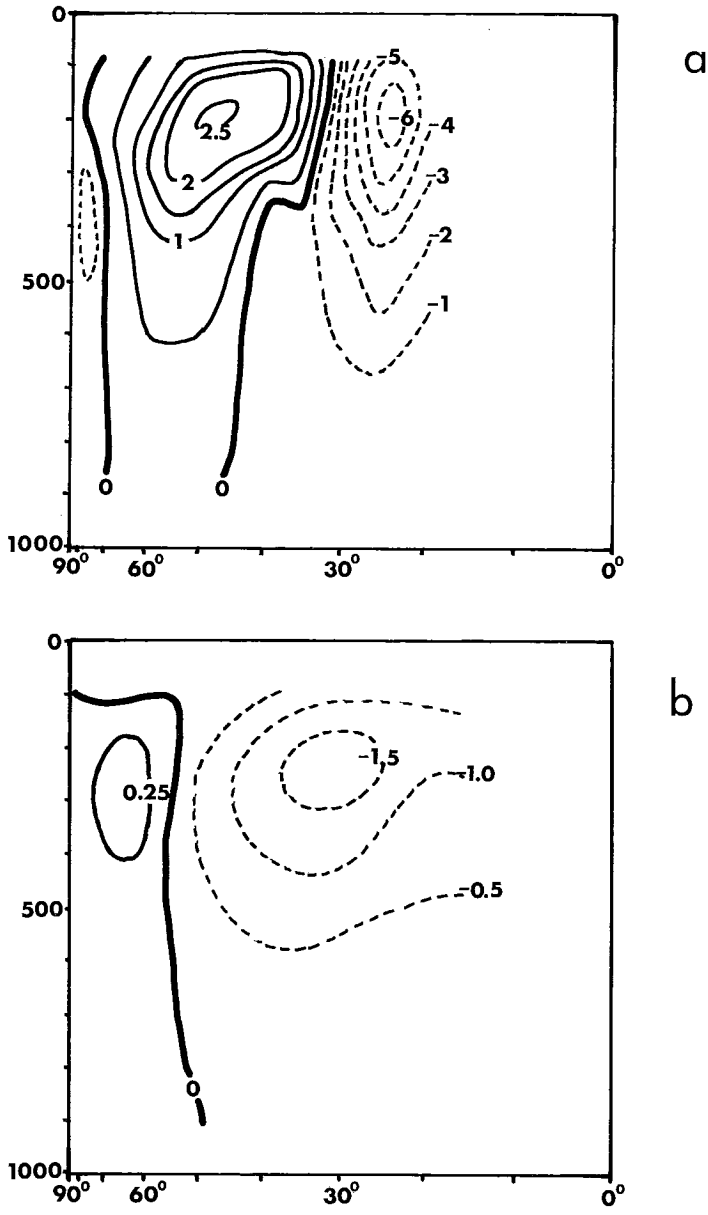

Fig. 4. The nongeostrophic zonal wind $[\bar{u}-\bar{u}_g]$ averaged for time and longitude. Unit: m s^{-1}.
a) monthly mean, high-index case (12/1965).
b) yearly mean, estimated by HOLOPAINEN [2].

scale fluctuations and contain »eddy statistics», the Reynolds' stresses $\overline{u'u'}$, $\overline{v'v'}$, $\overline{u'v'}$:

$$A_H = A_x i + A_y j \begin{cases} A_x = -\nabla \cdot \overline{u'V'} \\ A_y = -\nabla \cdot \overline{v'V'} \end{cases} \tag{3.2}$$

The eddy flux divergence term A_H is the horizontal forcing due to nonlinear turbulent interaction with the mean flow. In an SD model it must be related to the mean variables by some closure relations which are not known but may be diagnostic or prognostic.

The scales in (3.1) indicate a good geostrophic balance in monthly mean flow. However, if the terms labelled ? are small (as they probably are), there remains a triple balance between the horizontal advection, the remainder of the geostrophic terms and the interaction forcing A_H.

The horizontal distributions of the zonal component A_λ of the forcing vector A_H averaged vertically are shown in Fig. 2. for the two one-month periods. The local structure of A_λ is seen to be variable and the two cases are not very similar. The largest positive values occur in mid-latitudes, a fact which is more clearly seen in the zonal mean cross-section (Fig. 12a). In the absence of other forces this would indicate increasing mean zonal winds in mid-latitudes and decreasing mean winds in the subtropics: a »shift» of the mean wind maximum to the north. This is in good agreement with the $[\overline{u'v'}]$-values observed (OORT & RASMUSSON, [10]), A_λ being mainly composed of $-\partial/\partial\varphi\,[\overline{u'v'}]$. In the blocking case the largest values in magnitude occur in front of the blocking area and are positive. The effect of A_λ is thus to increase zonal wind in this area where the mean flow is mainly meridional.

The corresponding distributions for the meridional component A_φ are given in Fig. 3. In both cases A_φ is slightly larger in absolute values than A_λ, smoother and clearly zonal symmetric, the negative values occurring at lower latitudes. The surprising feature in the horizontal distributions of A_φ is that they seem quite similar in the two contrasting cases, and thus A_φ is not sensitive to the mean circulation pattern, unlike A_λ. The zonal mean values for A_λ and A_φ in the high-index case (Fig. 12a, b) show that the forcing is concentrated in the upper troposphere, where the winds are stronger.

If the ageostrophic mean zonal wind component averaged zonally is obtained from (3.1) the result, maintaining the large terms only, is:

$$[\bar{u} - \bar{u}_g] = \frac{1}{f}\left(-\frac{1}{a}\frac{\partial}{\partial\varphi}[\bar{v}^2] - \frac{\tan\varphi}{a}[\bar{u}^2 - \bar{v}^2] + [A_\varphi]\right) \tag{3.3}$$

The cross-section of the ageostrophic component (3.3) is shown in Fig. 4. for the high-index case together with corresponding yearly values calculated by HOLOPAINEN [2] (taken from LORENTZ [4], Fig. 9). The monthly values are larger, being up to -6 ms^{-1} in the upper troposphere at low latitudes, or about 10–15 % of the mean geostrophic winds. The supergeostrophic values in mid-latitudes are mainly due to positive A_φ-values and are larger than those found *e.g.* in OORT & RASMUSSON [10]. The mean circulation was, however, quite rapid in the high-index case.

The forcing thus seems to be important for the maintenance of monthly mean circulation and cannot be ignored in an SD model. One way of accounting for it is to form equations which describe the evolution of the Reynolds' stresses at fixed points. The resulting equations will, however, contain third moments (*e.g.* $\overline{u'u'v'}$, etc.) and an important question is then whether this closure problem can be solved by ignoring the third order terms if they appear small, or by parametrizing them by lower moments. This is discussed in the section on kinetic energy balance.

3.2 Kinetic energy

The importance of the eddy statistics for the maintenance of the mean flow and the fluctuation structure is perhaps better demonstrated in the local kinetic energy balance. Dividing the total kinetic energy $\frac{1}{2}\overline{V^2}$ into the kinetic energy of the time mean motion $K_m = \frac{1}{2}\bar{V}^2$ and the kinetic energy of the transient fluctuations $K_t = \frac{1}{2}\overline{V'^2}$ (the time domain, OORT [8]),

$$\tfrac{1}{2}\overline{V^2} = \tfrac{1}{2}\bar{V}^2 + \tfrac{1}{2}\overline{V'^2} = K_m + K_t \tag{3.4}$$

the total kinetic energy balance at any point (x, y, p, t) in the atmosphere is the sum of the partial balances of K_m and K_t:

$$\frac{\partial K_m}{\partial t} = -\nabla\cdot(\boldsymbol{H}_0 + \boldsymbol{H}_1) - \frac{\partial}{\partial p}(K_m\bar{\omega} + \overline{(\bar{V}'\cdot V')\omega'}) - \bar{V}\cdot\nabla\bar{\phi} + \bar{V}\cdot\bar{F} - C(K_m, K_t) \tag{3.5}$$

$$\frac{\partial K_t}{\partial t} = -\nabla\cdot(\boldsymbol{H}_2 + \boldsymbol{H}_3) - \frac{\partial}{\partial p}\overline{K_t\omega} - \overline{V'\cdot\nabla\phi'} + \overline{V'\cdot F'} + C(K_m, K_t) \tag{3.6}$$

(A) (B) (C) (D) (E)

where the terms (A) and (B) with notation

$$\begin{aligned}
\boldsymbol{H}_0 &= \tfrac{1}{2}(\bar{V}\cdot\bar{V})\,\bar{V} = K_m\bar{V}\\
\boldsymbol{H}_1 &= \overline{(\bar{V}\cdot V')\,V'}\\
\boldsymbol{H}_2 &= \tfrac{1}{2}(\overline{V'\cdot V'})\,\bar{V} = K_t\bar{V}\\
\boldsymbol{H}_3 &= \tfrac{1}{2}\overline{(V'\cdot V')\,V'}
\end{aligned} \tag{3.7}$$

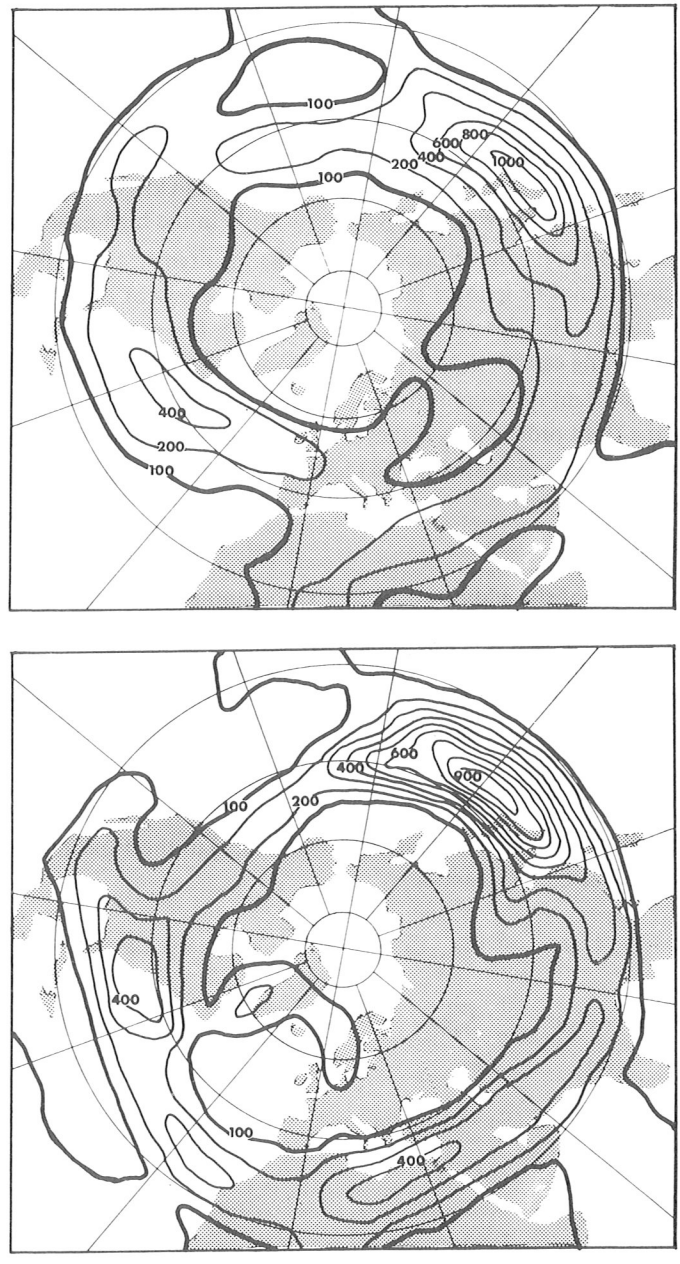

Fig. 5. Kinetic energy of the mean motion K_m averaged vertically. Unit: $m^2 s^{-2}$.

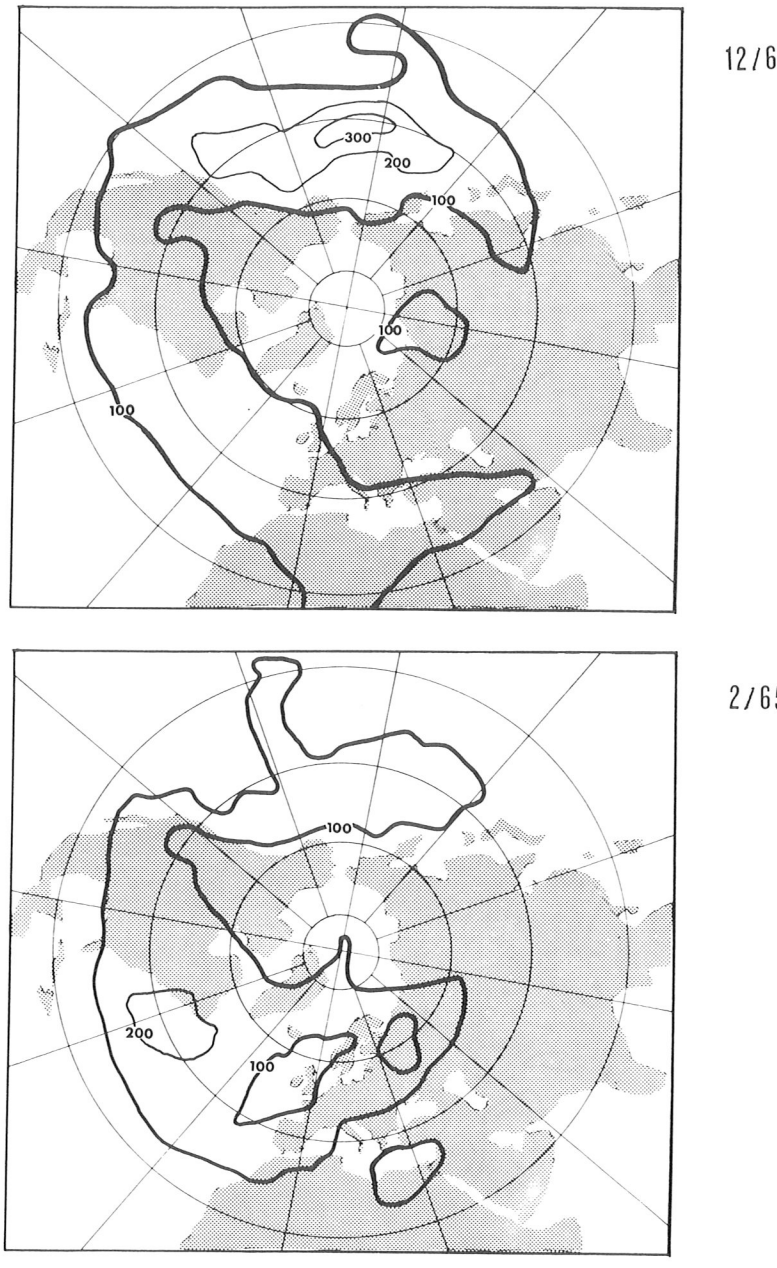

Fig. 6. Kinetic energy of the transient motion K_t averaged vertically. Unit: $m^2 s^{-2}$.

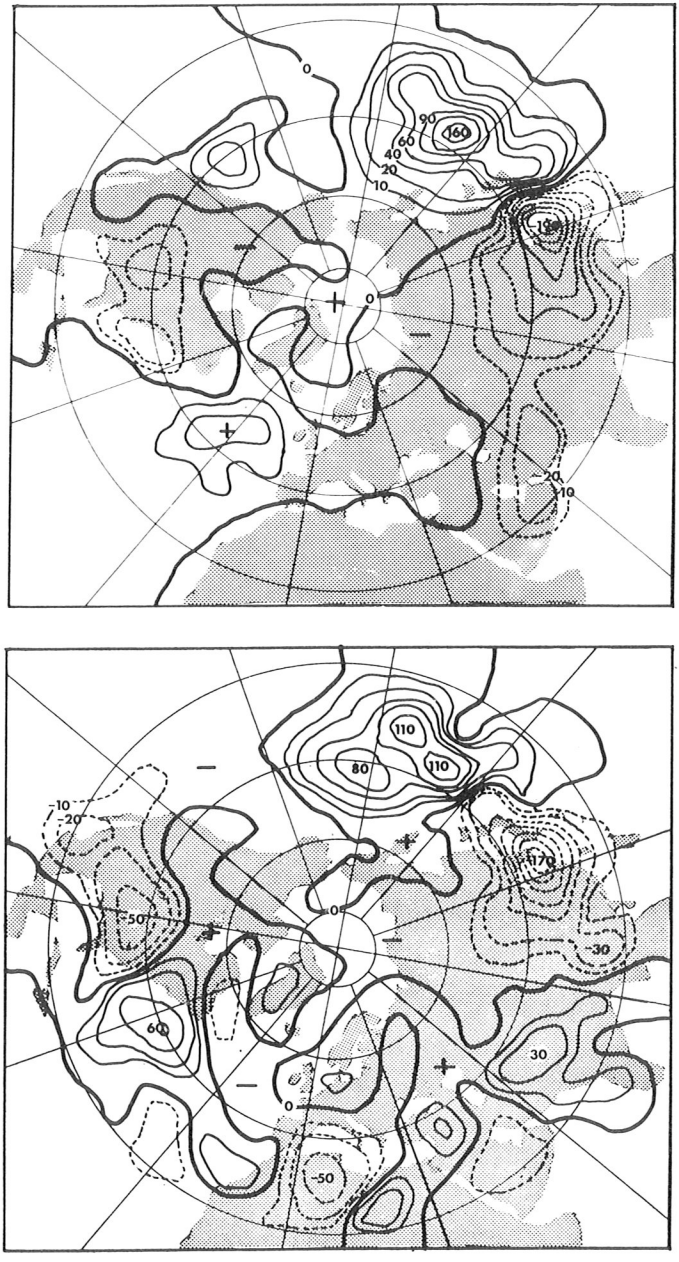

Fig. 7. Distribution $-\nabla \cdot H_0$ $(= -\nabla \cdot \frac{1}{2}|(\bar{V} \cdot \bar{V})\,\bar{V})$ averaged vertically. Unit: 10^{-4} W kg^{-1}.

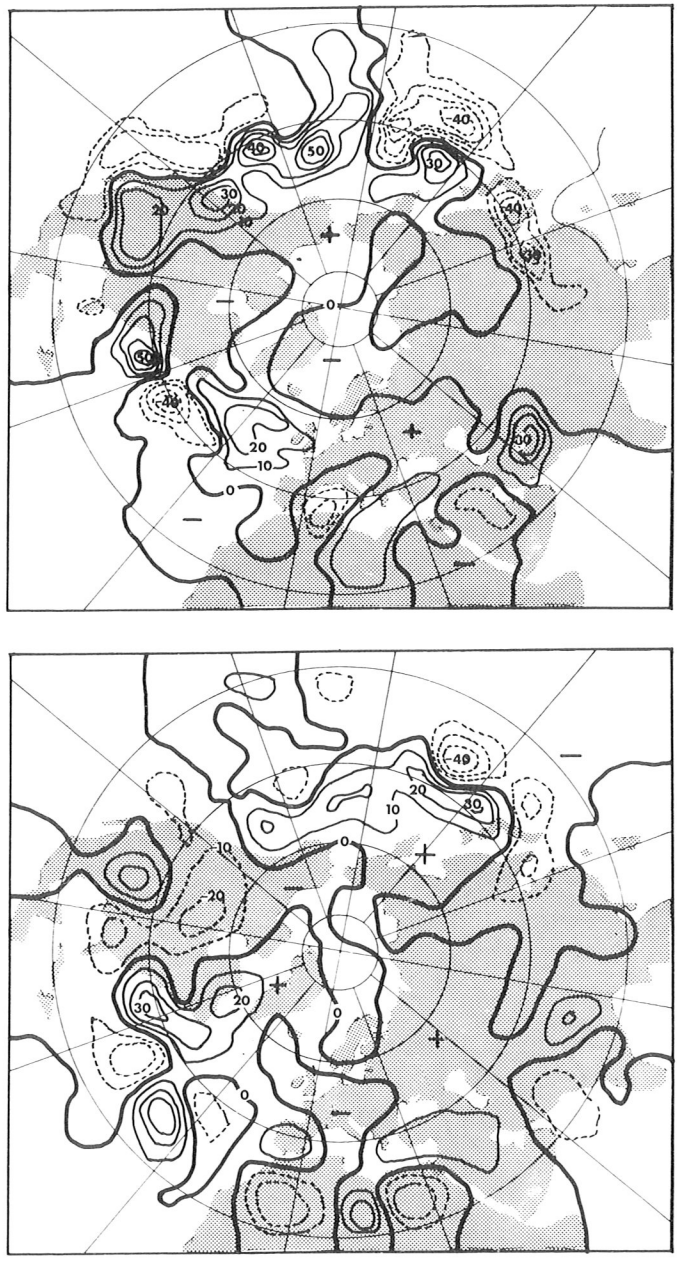

Fig. 8. Distribution of $-\nabla\cdot H_1$ $(= -\nabla\cdot(\overline{\bar{V}\cdot V)\,V'})$ averaged vertically. Unit: $10^{-4}\,\mathrm{Wkg}^{-1}$.

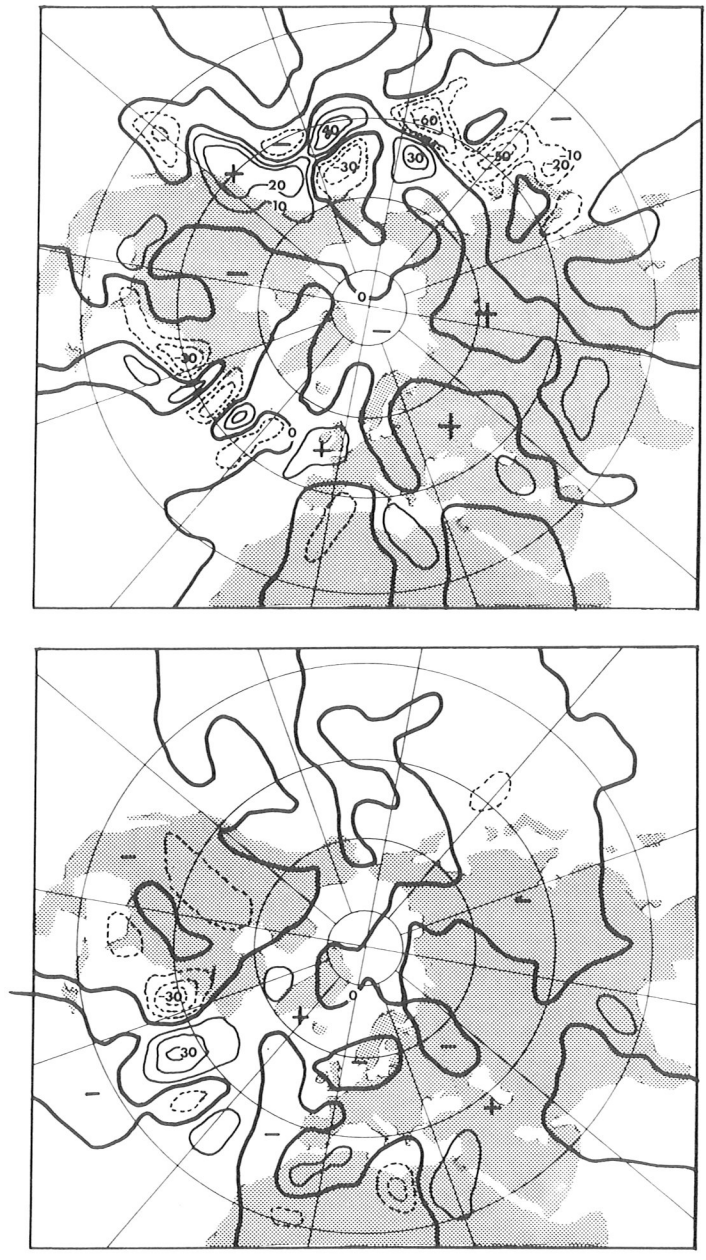

Fig. 9. Distribution of $-\nabla\cdot H_2$ $(= -\nabla\cdot\frac{1}{2}(\overline{V'\cdot V'})\,\bar{V})$ averaged vertically. Unit: $10^{-4}\,\mathrm{Wkg}^{-1}$.

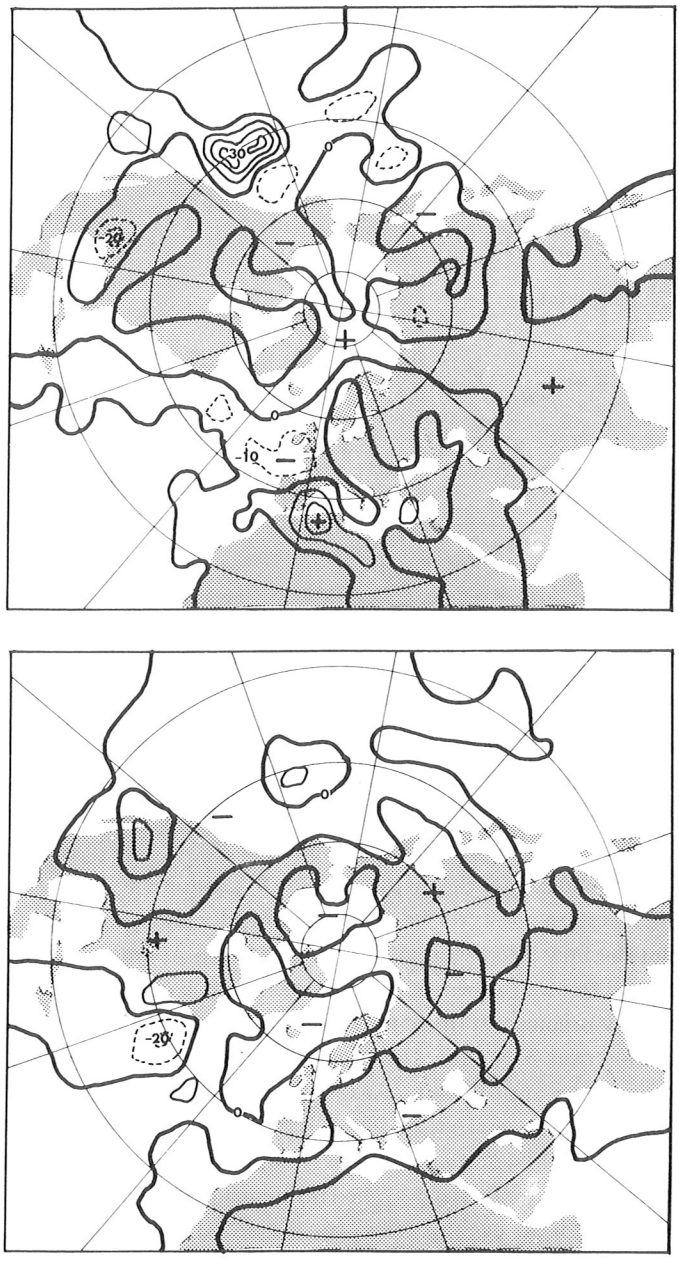

Fig. 10. Distribution of $-\nabla\cdot H_3$ $(= -\nabla\cdot\frac{1}{2}(\overline{V'\cdot V')V'})$ averaged vertically. Unit: 10^{-4} W kg^{-1}.

are associated with transports (horizontal and vertical convergences of energy fluxes), terms (C) represent the generation by horizontal pressure gradient forces, and terms (D) dissipation due to small-scale turbulence effects. Term (E) represents the conversion of K_m to K_t. It is defined positive, when K_m is converted to K_t, *i.e.* when fluctuations are »driven» at the expense of the mean motion. The conversion term is related to horizontal and vertical Reynolds' stresses:

$$C(K_m, K_t) = C_H(K_m, K_t) + C_V(K_m, K_t) \tag{3.8}$$

in spherical coordinates:

$$C_V(K_m, K_t) = -\overline{u'\omega'}\,\frac{\partial \bar{u}}{\partial p} - \overline{v'\omega'}\,\frac{\partial \bar{v}}{\partial p}$$

$$C_H(K_m, K_t) = -\frac{\overline{u'u'}}{a\cos\varphi}\,\frac{\partial \bar{u}}{\partial \lambda} - \frac{\overline{u'v'}}{a}\cos\varphi\,\frac{\partial}{\partial \varphi}\left(\frac{\bar{u}}{\cos\varphi}\right) - \frac{\overline{u'v'}}{a\cos\varphi}\,\frac{\partial \bar{v}}{\partial \lambda}$$

$$-\frac{\overline{v'v'}}{a}\cdot\frac{\partial \bar{v}}{\partial \varphi} + \overline{u'u'}\,\bar{v}\,\frac{\tan\varphi}{a}$$

$C_H(K_m, K_t)$ can also be written as

$$C_H(K_m, K_t) = -\nabla \cdot \boldsymbol{H}_1 - \bar{\boldsymbol{V}} \cdot \boldsymbol{A}_H \tag{3.9}$$

where the interaction vector $\boldsymbol{A}_H$ is given by (3.2). The equations (3.5), (3.6) could thus be written in an alternative form using (3.9), which might be physically clearer, but the present notation seems to have been adopted more widely.

Figures 5 and 6 show the vertical mean values of K_m and K_t in the two circulation types. In the high-index case the distribution of K_m is quite normal, showing two maxima at the western coasts of the oceans. In the blocking case the anticyclone centre divides the flow into two branches in the eastern Atlantic. The maxima of K_t may be expected to occur downstream from the maxima of K_m: although the disturbances may originate in the baroclinic regions near the mean jet core, they probably develop over 2–4 days. This is demonstrated in the K_t-patterns: the maxima are situated east of the maxima of K_m, the lag depending on the strength (and baroclinicity) of the mean flow. There is, however, only one clear maximum in both cases, and in the blocking case this maximum occurs just after the *less* intense mean jet above the Western Atlantic. The two branches of K_t around the blocking center agree well with the cyclone tracks for the period (PERRY, [7], Fig. 4b). These features of the transient disturbances should be reproduced by the parameterization schemes in areal SD models. The transport processes evidently have to be included in such schemes.

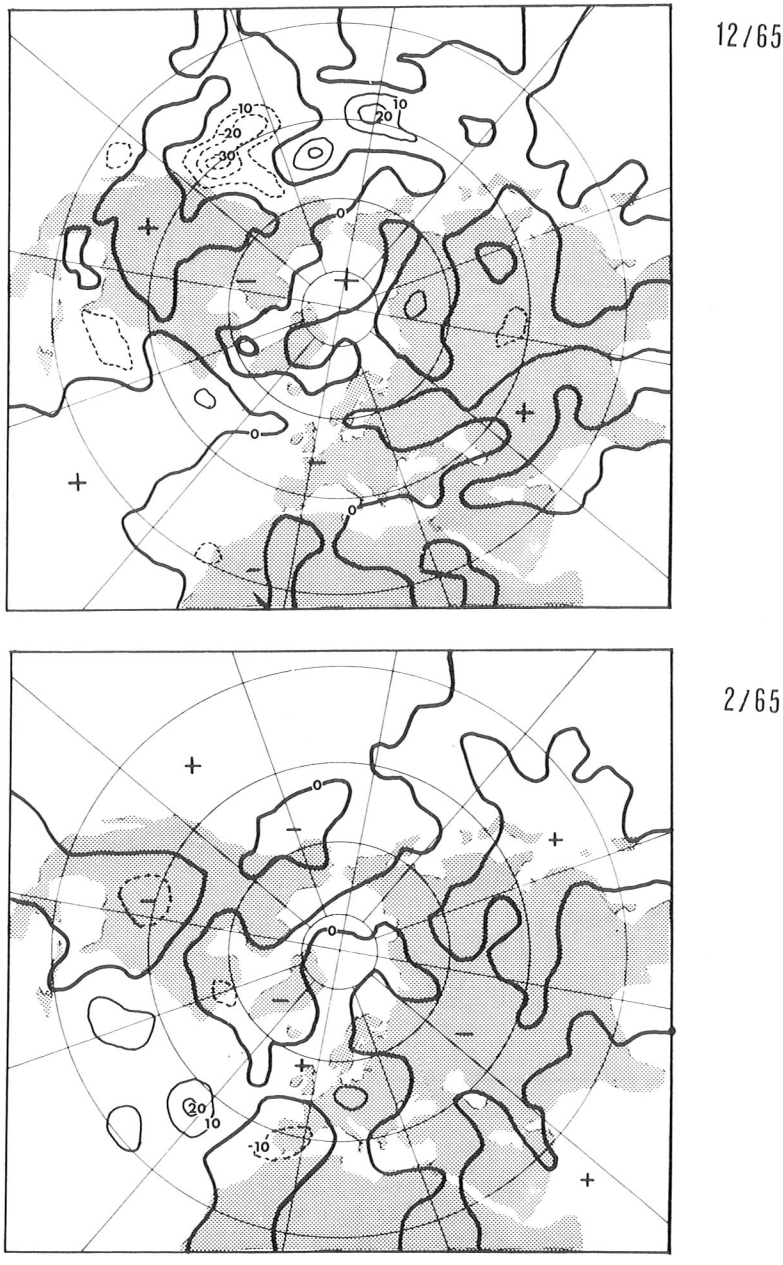

Fig. 11. Distribution of $C_H(K_m, K_t)$ averaged vertically. Unit: $10^{-4}\,\mathrm{W\,kg^{-1}}$.

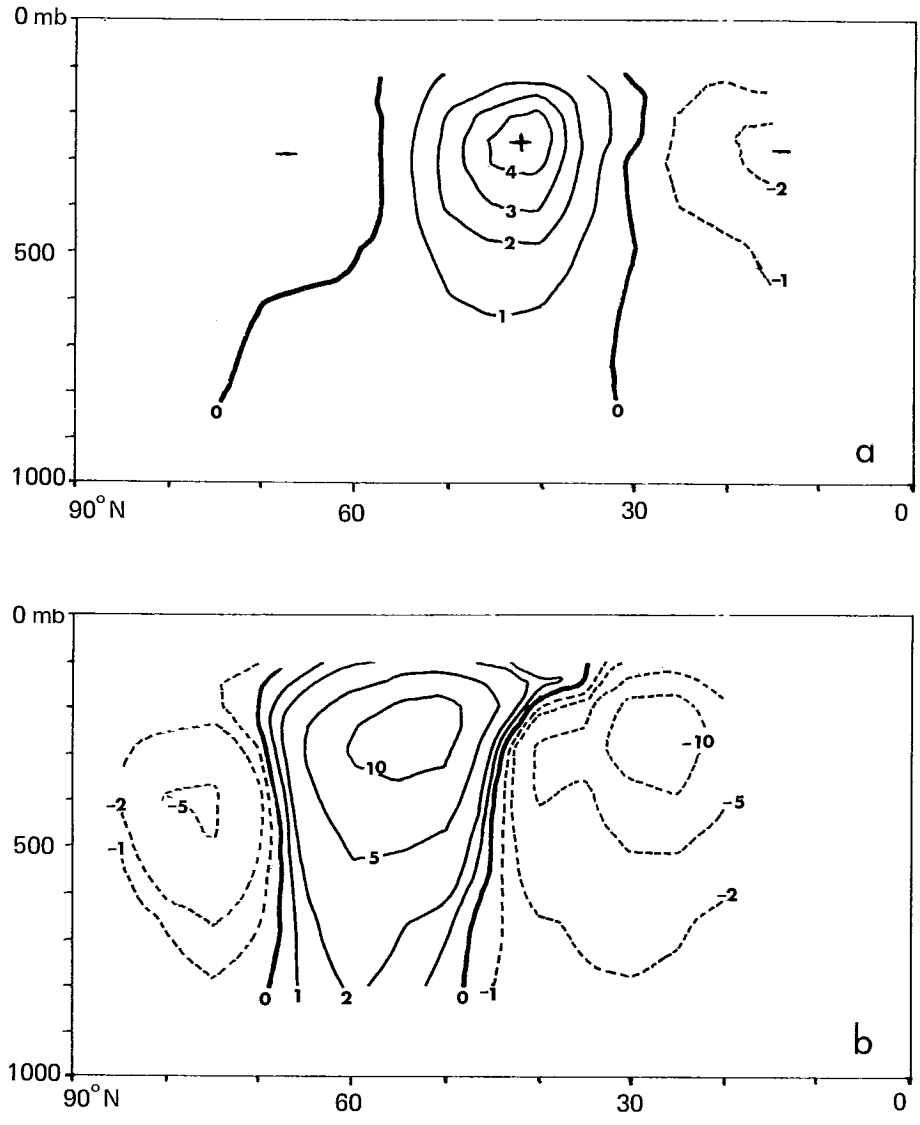

Fig. 12. Zonal averages for the high-index case (12/1965).
a) $[A_\lambda]$ unit: 10^{-5} m s^{-2}.
b) $[A_\varphi]$ unit: 10^{-5} m s^{-2}.
c) $[K_m]$, solid lines, $[K_t]$ dashed lines, unit: m^{2}s^{-2}.
d) $[C_H(K_m, K_t)]$, unit: 10^{-4} W kg^{-1}.

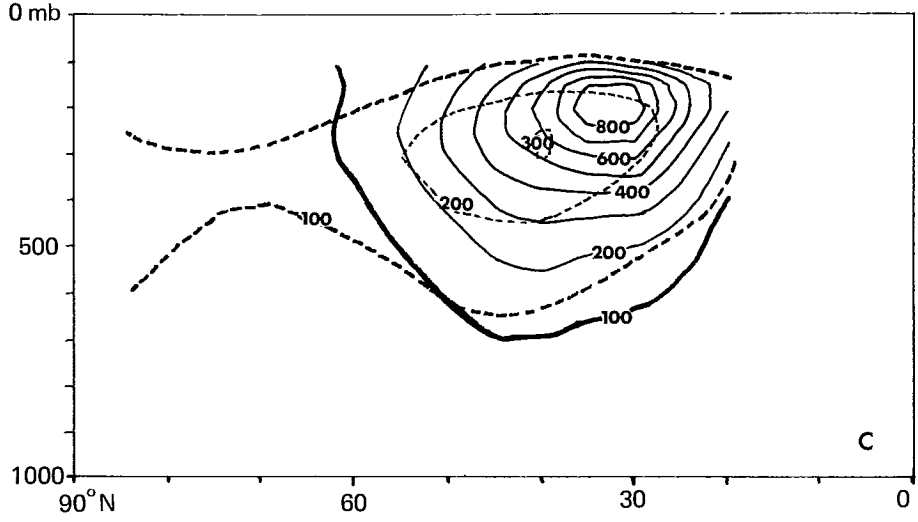
0 mb
500
1000
90°N
60
30
0
800
600
400
300
200
100
200
100
c

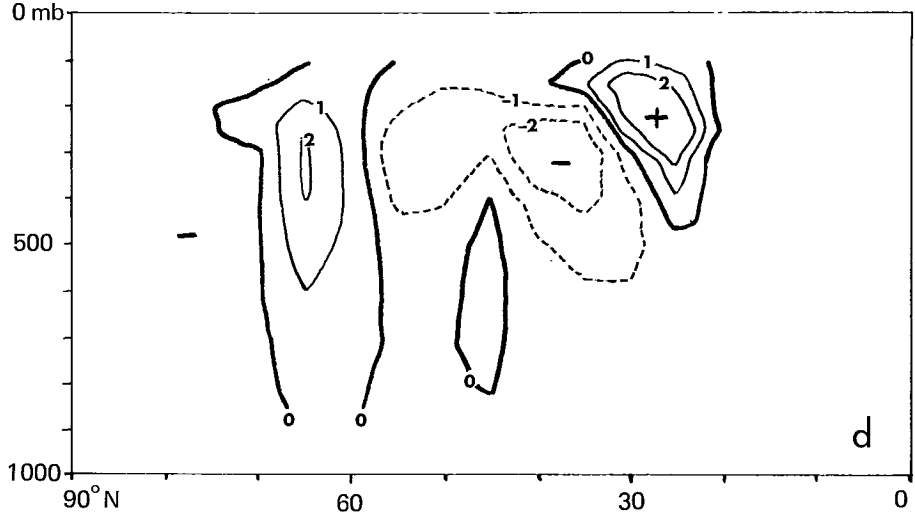
0 mb
500
1000
90°N
60
30
0
1
2
0
1
2
0
0
0
+
−
−
d

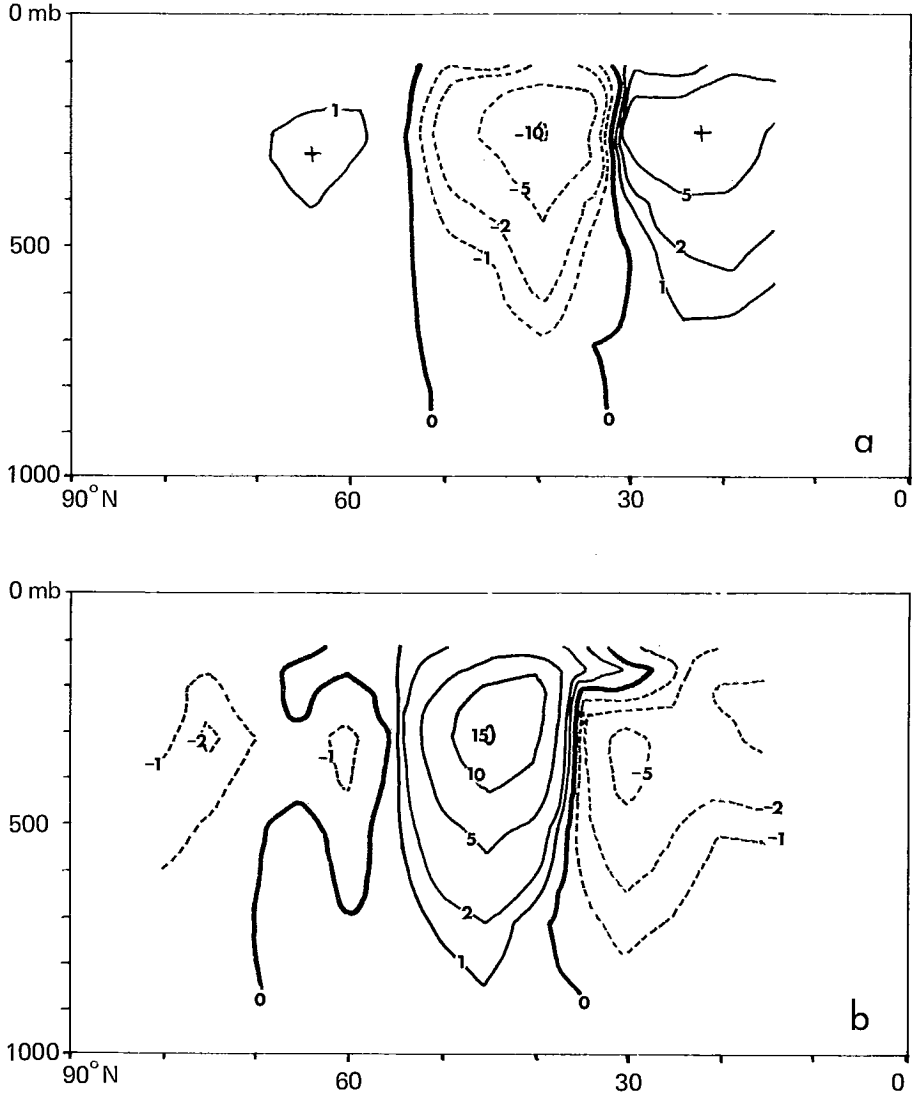

Fig. 13. Zonal averages for the high-index case (12/1965). Unit: 10^{-4} W kg^{-1}.
a) $[-\nabla \cdot H_0]$ b) $[-\nabla \cdot H_1]$ c) $[-\nabla \cdot H_2]$ d) $[-\nabla \cdot H_3]$

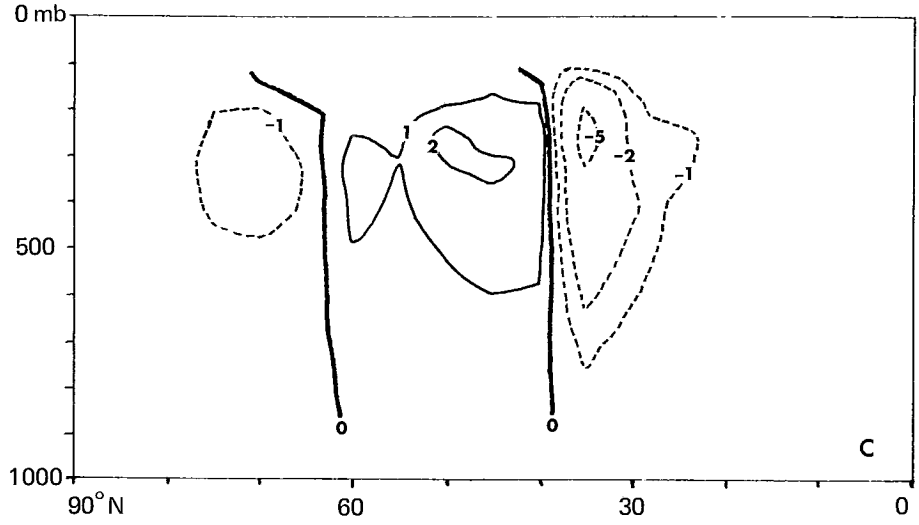
0 mb
500
1000
90° N
60
30
0
-1
1
2
-5
-2
-1
0
0
c

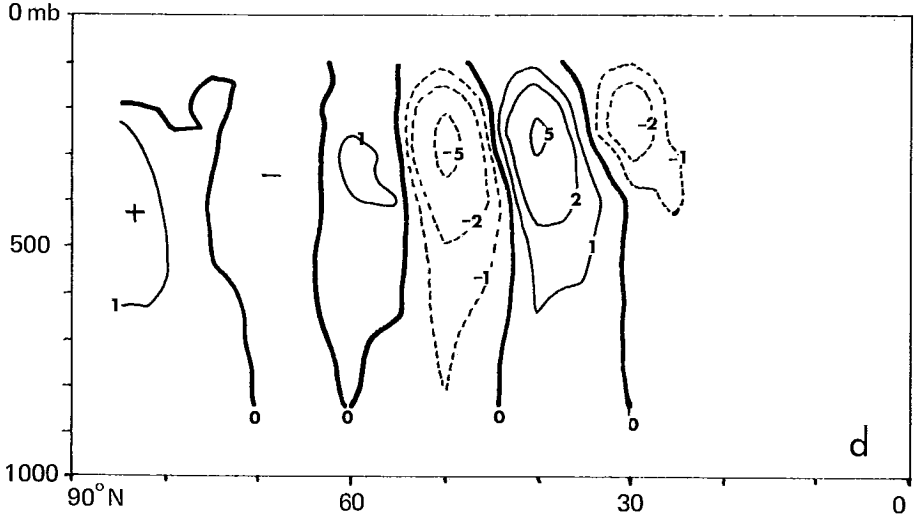
0 mb
500
1000
90° N
60
30
0
+
−
1
1
-5
5
-2
-2
2
-1
1
-1
0
0
0
0
d

In the present study the four flux divergence terms (3.7) and horizontal conversion term C_H (3.8) were calculated using geostrophic winds. As the local changes for monthly means are small, and probably also the terms connected with vertical motion and small-scale friction above the boundary layer, the generation terms (which cannot be computed from geostrophic winds) may be approximated from the quasi-balance:

$$0 = -\nabla\cdot(\boldsymbol{H}_0 + \boldsymbol{H}_1) - \bar{\boldsymbol{V}}\cdot\nabla\bar{\phi} - C_H(K_m, K_t) \qquad \text{above the boundary layer} \qquad (3.5)'$$

$$0 = -\nabla\cdot(\boldsymbol{H}_2 + \boldsymbol{H}_3) - \overline{\boldsymbol{V}'\cdot\nabla\phi'} + C_H(K_m, K_t) \qquad (3.6)'$$

The vertical mean values of the four energy flux terms are shown in Figs. 7–10, in units 10^{-4} W kg^{-1}. All the distributions show large longitudinal variability. Averaged zonally, $-\nabla\cdot\boldsymbol{H}_0$ and $-\nabla\cdot\boldsymbol{H}_1$ (Fig. 13a,b) seem to balance out quite well, but locally this is not the case. The mean advection of the kinetic energy of mean motion $-\nabla\cdot\boldsymbol{H}_0$ includes only mean variables, which are straightforwardly computable in SD or »mean motion» models. It is largest in magnitude, positive over oceans and negative over continents. $-\nabla\cdot\boldsymbol{H}_1$ is more zonal symmetric. It is expected to correlate with A_λ according to (3.9); this is verified by comparing the two distributions (Figs. 2 and 8). In fact, the fields $-\nabla\cdot\boldsymbol{H}_1$ and $\bar{\boldsymbol{V}}\cdot\boldsymbol{A}_H$ are quite similar and the conversion term C_H remains smaller. The distribution of C_H (Fig. 11) is quite variable but mainly negative, the overall average being about -0.2 W m^{-2} for the Northern Hemisphere north of 20°N above the boundary layer. A value of -0.3 W m^{-2} has been presented for yearly means using observed winds between 100 and 1000 mb (HOLOPAINEN, [3]). Fluctuating motion thus generally feeds energy to the mean motion in the time domain, too. This negative viscosity is not, however, uniform: sufficiently strong disturbances (large K_t) seem to draw energy from the mean flow as C_H is consistently positive in the areas of maximal monthly K_t.

For the maintenance of K_m the generation term $-\bar{\boldsymbol{V}}\cdot\nabla\bar{\phi}$ must balance eq. (3.5):

$$-\bar{\boldsymbol{V}}\cdot\nabla\bar{\phi} = \nabla\cdot\boldsymbol{H}_0 - \bar{\boldsymbol{V}}\cdot\boldsymbol{A}_H \qquad (3.5)''$$

Using geostrophic winds for the terms on the right-hand side is equivalent to using wind for the left-hand side approximated from the equation of motion (3.1):

$$\bar{\boldsymbol{V}} = \bar{\boldsymbol{V}}_g + \frac{k\times}{f}((\bar{\boldsymbol{V}}_g\cdot\nabla)\,\bar{\boldsymbol{V}}_g - \boldsymbol{A}_H) = \bar{\boldsymbol{V}}_g + \frac{k\times}{f}(\bar{\zeta}_g k\times\bar{\boldsymbol{V}}_g + \nabla\tfrac{1}{2}\bar{\boldsymbol{V}}_g^2 - \boldsymbol{A}_H)$$

(cf. 3.3), where $\bar{\zeta}_g$ is mean geostrophic vorticity. (3.5)" is thus a »quasigeostrophic» approximation to the generation of K_m. The generation term is in both cases negative

above oceans (sink of K_m) and positive over continents (source of K_m), which is consistent with the ageostrophic wind structure often observed in large-scale confluent and diffluent height field patterns.

The transport terms for the maintenance of K_t; $-\nabla\cdot\boldsymbol{H}_2$ and $-\nabla\cdot\boldsymbol{H}_3$, are found to be slightly smaller than the corresponding terms for K_m. They are quite variable locally and all three terms of the budget of K_t calculated seem to be locally important.

If we finally discuss the third order term $-\nabla\cdot\boldsymbol{H}_3$ we find it is generally small but not negligible compared with other terms, locally variable, not clearly related to the mean flow quantities and quite different in the two cases. As this term is the convergence of the horizontal transient kinetic energy flux associated with transient motion, it might be expected that if the disturbances tend to diffuse K_t, $-\nabla\cdot\boldsymbol{H}_3$ would be correlated to $\nabla^2 K_t$. The negative maxima of $-\nabla\cdot\boldsymbol{H}_3$ are indeed situated in areas of the local maxima of K_t (where $\nabla^2 K_t$ is negative) in both cases. This gives faint support to a closure scheme using diffusion concepts to third order terms, but the total correlations $r(\nabla\cdot\boldsymbol{H}_3, \nabla^2 K_t)$ are almost zero. This agrees qualitatively with results obtained by van den DOOL [1] for the Atlantic area 500 mb level and MÄLKKI [5] for sea currents in a small area of the Baltic Sea.

The balance of the total kinetic energy, which is the sum of (3.5) and (3.6), is dependent on all four energy fluxes in the monthly scale, although the terms with higher moments are smaller. The division into an arithmetic mean and deviations from it is, however, quite crude as the deviations may be due to different physical reasons. Another drawback, apart from the geostrophic wind approximation, is the fact that the regions of maximum values in many of the fields calculated are situated above oceans where the numerical analyses used were more or less affected by the normal and model-predicted values because of few observations.

4. *Conclusion*

The significance of transient horizontal eddies (»large-scale turbulence») for the maintenance of mean and transient modes of atmospheric motion for a one-month averaging period is demonstrated in the present study.

For the mean meridional motion the nonlinear zonal interaction force A_φ is found to be quite zonal symmetric and fairly independent of the mean circulation. On the other hand, the corresponding meridional forcing component A_λ is different in both cases studied.

In the balance of kinetic energy budget for a one-month scale all the terms presented are longitudinally quite variable and the local balance depends on energy fluxes, local generation, dissipation and transform terms. However, terms loaded

with higher eddy statistics (»more primes») are smaller and may perhaps be neglected as a zeroth approximation for local SD models. A first approximation according to the present results might be diffusion-like parameterization for third order statistics, although this has to be checked by other studies using wind observations.

A general feature of our atmosphere, well indicated in the present study, too, is the most intense turbulence even on a large scale above oceans. Unfortunately the present observational network is least dense in these areas. The GARP experiments will thus be valuable in providing data for further studies on these important but uninhabited »information deserts».

REFERENCES

1. DOOL, H.M. van den, 1975: Three studies on spectral structures of the horizontal atmospheric motion in the time domain. *Doctoral thesis, University of Utrecht.*
2. HOLOPAINEN, E.O., 1966: Some dynamic applications of upper-wind statistics. *Finnish Met. Off. Contrib.* **62**, 22 pp.
3. –»–, 1975: Diagnostic studies on the interaction between the time-mean flow and the large-scale transient fluctuations in the atmosphere. *Report 8, Dept. of Meteorology, University of Helsinki,* 14 pp.
4. LORENTZ, E.N., 1967: *The nature and theory of the general circulation of the atmosphere.* WMO No. 218, TP. 115.
5. MÄLKKI, P., 1975: On the variability of currents in a coastal region of the Baltic Sea. *Merentutkimuslaitoksen julkaisu* No. 240, 3–56.
6. MURRAY, R., 1966: The blocking patterns of February 1965 and a good pressure analogue. *Weather,* **21**, 66–69.
7. PERRY, A.H., 1968: Turbulent heat flux patterns over the North Atlantic during recent winter months. *Met. Magazine,* **97**, 246–254.
8. OORT, A.H., 1964: On estimates of the atmospheric energy cycle. *Mon. Weath. Rev.,* **92**, 483–493.
9. OORT, A.H. and PEIXOTO, J., 1975: The annual cycle of the energetics of the atmosphere on a planetary scale. *J. Geophys. Res.,* **79**, 2706–2720.
10. OORT, A.H. and RASMUSSON, E.H., 1971: Atmospheric circulation statistics. *NOAA Professional Paper 5.*
11. SALTZMAN, B. and A.D. VERNEKAR, 1971: An equilibrium solution for the axially symmetric component of the earth's macroclimate. *J. Geophys. Res.,* **76**, 1498–1524.
12. STARK, L.P., 1965: The weather and circulation of February 1965: Strong Atlantic blocking. *Mon. Weath. Rev.,* **93**, 336–342.
13. WILLSON, M.A.G., 1973: Statistical-dynamical modelling of the atmosphere. *Commonw. Met. Res. Centre, Melbourne, Int. Sci. Rep.*